Cascaded Nonlinear Control Design for Highly Underactuated Balance Robots

Feng Han and Jingang Yi

Abstract—This paper presents a nonlinear control design for highly underactuated balance robots, where the number of unactuated degree-of-freedom is greater than that of actuated one. To address the challenge of simultaneously trajectory tracking and balancing, the control converts a robot dynamics into a series of cascaded subsystems and each of them is considered virtually actuated. We sequentially design and update the virtual and actual control inputs to incorporate the balance task such that the unactuated coordinates are balanced to their instantaneous equilibrium. The closed-loop dynamics are shown to be stable and the tracking errors exponentially converge towards a neighborhood near the origin. The simulation results demonstrate the effectiveness of the proposed control design by using a triple-inverted pendulum cart system.

I. Introduction

Underactuated robots have less number of control inputs than that of the degree-of-freedom (DOF). Control design for underactuated balance robots faces the challenge of limited control actuation for simultaneous trajectory tracking and platform balance. Most existing works focus on underactuated balance systems with more actuated coordinates than unactuated ones. For instance, a cart-pole system has one input with one unacuated DOF [1], [2], a bipedal robot has four inputs with one unacuated DOF [3], and an autonomous bicycle robot has two inputs and one unacuated DOF [4], [5], to name a few examples. There are various well-developed control frameworks for those including the external and internal convertible form-based control (i.e., EIC-based control) [6], orbital stabilization [7], [8], energyshaping based control [9], etc. Both the model-based control and machine learning-based control approaches are extensively studied [2], [10]. However, for highly underactuated balance robots with more unactuated coordinates than actuated ones, such as a triple passive inverted pendulum on a controlled cart (i.e., one input with three unactuated DOFs), those control approaches do not work properly.

For highly underactuated balance robots, the inherently unstable property and coupled dynamics impose great challenges in control system design [11], [12]. With limited available control actuation, there exist great competing tasks between trajectory tracking and balance stabilization. To reduce the design complexity, most of the existing works focus on stabilization control only. Linearization of nonlinear system and pole placement/linear quadratic regulator (LQR) techniques are among popular methods [12]–[15]. The work

This work was supported in part by the US NSF under award CNS-1932370.

in [13] presented an LQR-based robust control for a triple-invented pendulum cart system and a fault tolerant control was proposed for a double-inverted pendulum cart system using a linearized model [15]. In [16], the authors enhanced the inversion-based approach (e.g., [17]) towards the stabilization of a periodic orbit of a multi-link triple pendulum on a cart. However, simultaneous control of trajectory tracking and platform balance remains a challenge for highly underactuated balance robots.

Among the aforementioned control methods, the EIC-based control has been demonstrated as an effective approach to achieve tracking and balance. The previously developed EIC-based control was designed for various types of underactuated balance robots that have more numbers of actuated than unactuated DOFs [2], [4], [10], [18]. The unstable and unactuated subsystem is balanced onto a balance equilibrium manifold (BEM) and trajectory tracking and platform balance control are achieved simultaneously. Given such an attractive feature, the EIC-based control can be potentially revised for highly underactuated balance robots.

The EIC-based control design embeds the balance task into the trajectory tracking. The BEM is associated with the actuated subsystem motion effect and the motion of the actuated subsystem is used as a virtual input to drive the unactuated subsystem to its BEM. Inspired by such an observation, we propose a cascaded EIC form (i.e., CEIC) that transforms a highly underactuated balance system into a series of cascaded subsystems, which are virtually actuated. We sequentially estimate and obtain the BEM and then update the control input of the subsystem. Each subsystem has been shown under active control design. Trajectory tracking and balance control can be achieved. We illustrate and demonstrate the CIEC-based control through an example of a triple-inverted pendulum on a cart. The main contribution of this work is the proposed new cascaded control framework for highly underactuated balance robots. We also for the first time reveal the controllable condition of the highly underactuated balance robots.

II. HIGHLY UNDERACTUATED BALANCE ROBOTS

A. Robot Dynamics

Let the generalized coordinates of an underactuated balance robot be $\mathbf{q} = [q_1 \cdots q_{n+m}]^T \in \mathbb{R}^{n+m}, \ n,m \in \mathbb{N}$. We partition \mathbf{q} into $\mathbf{q} = [\mathbf{q}_a^T \ \mathbf{q}_u^T]^T$ with actuated coordinate $\mathbf{q}_a \in \mathbb{R}^n$ and unactuated $\mathbf{q}_u \in \mathbb{R}^m$. The robot dynamics for actuated and unactuated subsystems are [19]

$$S_a: D_{aa}\ddot{q}_a + D_{au}\ddot{q}_u + C_a\dot{q} + G_a = u, \qquad (1a)$$

$$S_u: D_{ua}\ddot{q}_a + D_{uu}\ddot{q}_u + C_u\dot{q} + G_u = 0, \qquad (1b)$$

F. Han and J. Yi are with the Department of Mechanical and Aerospace Engineering, Rutgers University, Piscataway, NJ 08854 USA (e-mail: fh233@scarletmail.rutgers.edu; jgyi@rutgers.edu).

where D(q), $C(q,\dot{q})$ and G(q) are the inertia, Coriolis and gravity matrices, respectively. The subscripts aa (uu) and ua and au indicate the variables related to the actuated (unactuated) coordinates and coupling effects, respectively. For the convenience of representation, the dependence of matrices D, C, and G on q and \dot{q} is dropped and we denote $H_a = C_a \dot{q} + G_a$ and $H_u = C_u \dot{q} + G_u$.

The unactuated dynamics S_u in (1b) is intrinsically unstable. The control goal for $S = \{S_a, S_u\}$ is to track the given trajectory q_a^d for S_a while balance the unstable S_u around unknown equilibria. Most of the existing works focus on the robot dynamics with $n \geq m$, that is, more actuated than unactuated DOFs. In this work, we consider highly underactuated balance robots, i.e., n < m. With less control actuation than the number of unactuated DOFs, it becomes challenging for simultaneously trajectory tracking and platform balance control design [16].

B. EIC-Based Tracking and Balance Control

We first present the EIC-based control and discuss its limitations for highly underactuated balance robot control. Given desired trajectory q_a^d for S_a , we temporarily neglect the dynamics of S_u and the tracking control is designed as

$$\boldsymbol{u}_a^{\text{ext}} = \boldsymbol{D}_{aa} \boldsymbol{v}_a^{\text{ext}} + \boldsymbol{D}_{au} \ddot{\boldsymbol{q}}_u + \boldsymbol{H}_a, \tag{2}$$

where $v_a^{\rm ext} = \ddot{q}_a^d - k_{p1}e_a - k_{d1}\dot{e}_a$ is an auxiliary control design. $e_a = q_a - q_a^d$ is the tracking error and $k_{p1}, k_{d1} \in \mathbb{R}^{n \times n}$ are control gains.

The q_u coordinate should be stabilized onto the BEM. The BEM is defined as the instantaneous equilibrium of q_u as

$$\mathcal{E} = \left\{ \boldsymbol{q}_u^e : \Gamma(\boldsymbol{q}_u; \boldsymbol{v}_a^{\mathrm{ext}}) = \boldsymbol{0}, \dot{\boldsymbol{q}}_u = \ddot{\boldsymbol{q}}_u = \boldsymbol{0} \right\},$$
 (3)

where $\Gamma(q_u; v_a^{\mathrm{ext}}) = D_{uu}\ddot{q}_u + D_{ua}v_a^{\mathrm{ext}} + H_u$. The equilibrium q_u^e is obtained by solving $\Gamma(q_u; v_a^{\mathrm{ext}})\big|_{\dot{q}_u=\ddot{q}_u=0}=0$. Using $q_u^e \in \mathcal{E}$ as a targeted reference, \ddot{q}_a profile is redesigned such that under $\ddot{q}_a, q_u \to q_u^e$. The control is updated by incorporating the \mathcal{S}_u dynamics as

$$\boldsymbol{v}_{a}^{\mathrm{int}} = -\boldsymbol{D}_{ua}^{+}(\boldsymbol{H}_{u} + \boldsymbol{D}_{uu}\boldsymbol{v}_{u}^{\mathrm{int}}), \tag{4}$$

where $v_u^{\text{int}} = \ddot{q}_u^e - k_{p2}e_u - k_{d2}e_u$, $D_{ua}^+ = (D_{ua}^TD_{ua})^{-1}D_{ua}^T$ is the generalized inverse of D_{ua} , $e_u = q_u - q_u^e$ and $k_{p2}, k_{d2} \in \mathbb{R}^{m \times m}$ are control gains. With the design (4), the final control becomes

$$\boldsymbol{u}_{a}^{\mathrm{int}} = \boldsymbol{D}_{aa}\boldsymbol{v}_{a}^{\mathrm{int}} + \boldsymbol{D}_{au}\ddot{\boldsymbol{q}}_{u} + \boldsymbol{H}_{a}. \tag{5}$$

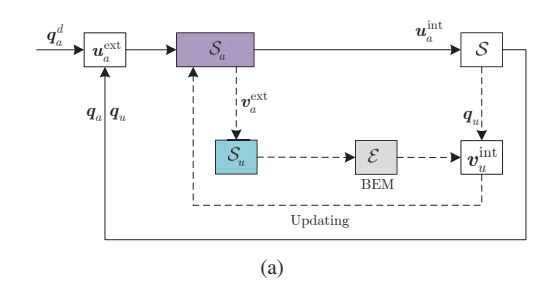
The above sequentially designed control, known as EIC-based control, aims to achieve tracking of S_a and balance of S_u simultaneously [6]. Fig. 1(a) illustrates the design flowchart of the EIC-based control.

We now inspect the closed-loop dynamics under the EIC-basad control. Plugging u_a^{int} into dynamics S_u , we obtain

$$\ddot{q}_{u} = -D_{uu}^{-1}(D_{ua}\ddot{q}_{a} + H_{u})
= -D_{uu}^{-1} \left[-D_{ua}D_{ua}^{+}(H_{u} + D_{uu}v_{u}^{\text{int}}) + H_{u} \right].$$
(6)

Since $D_{ua} \in \mathbb{R}^{m \times n}$ and n < m, we have $D_{ua}D_{ua}^+ \in \mathbb{R}^{m \times m}$ and $\operatorname{rank}(D_{ua}D_{ua}^+) = n < m$. Therefore, part of the

control effect of $v_u^{\rm int}$ would not appear and the nonlinearity term H_u cannot be fully canceled at all dimensions. The unactuated subsystem \mathcal{S}_u does not approach to \mathcal{E} as the design goal and the balance would not be guaranteed for highly underactuated balance robot.



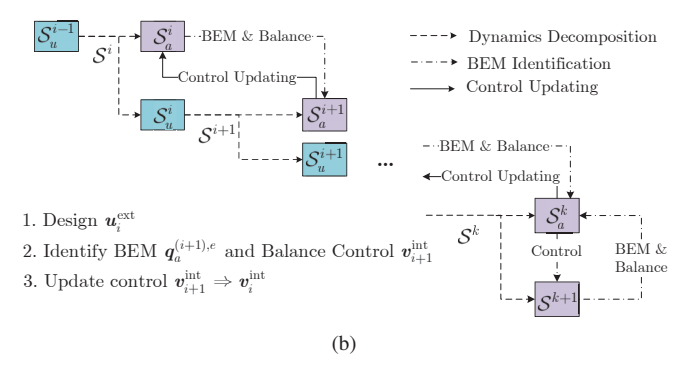


Fig. 1. Illustrative diagram of control design for underactuated baleen system $\mathcal S$ based on EIC structure. (a) EIC-based control design. (b) CEIC-based control design.

III. CASCADED EIC FORM FOR HIGHLY UNDERACTUATED SYSTEM

The EIC-based control has been successfully demonstrated for underactuated balance robots with $n \geq m$ [20]. In EIC-based control, the designed motion effects $\ddot{q}_a = v_a^{\rm int}$ is used as a virtual control when incorporating the balance control $v_u^{\rm int}$ into final control; see (4). However, the \mathcal{S}_u dynamics with respect to \ddot{q}_a is indeed an underactuated system with m coordinates and n inputs. For such an underactuated subsystem, we can perform the EIC-based control again to \mathcal{S}_u . Following such an inspiration, we formally present the CEIC design.

The S_a dynamics under the control u can be solved as

$$\ddot{q}_a = D_{aa}^{-1} (u - D_{au} \ddot{q}_u - H_a).$$
 (7)

Plugging (7) into (1b) yields

$$S^{1}: D^{(1)}\ddot{a}^{(1)} + H^{(1)} = B^{(1)}u, \tag{8}$$

where $q^{(1)}=q_u$ and $D^{(1)}=D_{uu}-D_{ua}D_{aa}^{-1}D_{au}$, $H^{(1)}=H_u-D_{ua}D_{aa}^{-1}H_a$, $B^{(1)}=-D_{ua}D_{aa}^{-1}$. We note $D_{ua}\in\mathbb{R}^{m\times n}$ and $B^{(1)}\in\mathbb{R}^{m\times n}$. Equation (8) represents another underactuated system with m generalized coordinates and n control inputs.

We partition the $q^{(1)}$ coordinates into two parts as $q^{(1)} = \left[(q_a^{(1)})^T \ (q_u^{(1)})^T \right]^T$, where $q_a^{(1)}$ denotes the first n unactuated coordinates, such that $\dim(q_a^{(1)}) = n$, $\dim(q_u^{(1)}) = n$

(9a)

 $\mathcal{S}_{a}^{1}: D_{aa}^{(1)}\ddot{q}_{a}^{(1)} + D_{aa}^{(1)}\ddot{q}_{a}^{(1)} + H_{a}^{(1)} = B_{a}^{(1)}u,$

$$S_u^1: D_{ua}^{(1)} \ddot{q}_a^{(1)} + D_{uu}^{(1)} \ddot{q}_u^{(1)} + H_u^{(1)} = B_u^{(1)} u, \qquad (9b)$$

where $D^{(1)}$, $H^{(1)}$ and $B^{(1)}$ are partitioned into block matrices with appropriate dimensions. Similar to (1), (9) is in the form of an underactuated robot model. The input matrix $B^{(1)}$ in S^1 is no longer a constant and the selection of $\dim(u) = n$ generalized coordinates as the actuated ones out of $q^{(1)}$ is arbitrary, as long as $\operatorname{rank}(B_a^{(1)}) = n$.

We solve $\ddot{q}_a^{(1)} = D_{aa}^{(1)} \left(B_a^{(1)} u - D_{au}^{(1)} \ddot{q}_u^{(1)} - H_a^{(1)} \right)$ using \mathcal{S}_a^1 . Substituting $\ddot{q}_a^{(1)}$ into \mathcal{S}_u^1 yields

$$S^2: D^{(2)}\ddot{q}^{(2)} + H^{(2)} = B^{(2)}u,$$

where $\boldsymbol{q}^{(2)} = \boldsymbol{q}_u^{(1)}$ and $\boldsymbol{D}^{(2)} = \boldsymbol{D}_{uu}^{(1)} - \boldsymbol{D}_{ua}^{(1)} \left(\boldsymbol{D}_{aa}^{(1)}\right)^{-1} \boldsymbol{D}_{au}^{(1)},$ $\boldsymbol{H}^{(2)} = \boldsymbol{H}_u^{(1)} - \boldsymbol{D}_{ua}^{(1)} \left(\boldsymbol{D}_{aa}^{(1)}\right)^{-1} \boldsymbol{H}_a^{(1)},$ and $\boldsymbol{B}^{(2)} = \boldsymbol{B}_u^{(1)} - \boldsymbol{D}_{ua}^{(1)} \left(\boldsymbol{D}_{aa}^{(1)}\right)^{-1} \boldsymbol{B}_a^{(1)}.$ If $\dim(\boldsymbol{q}_u^{(2)}) > \dim(\boldsymbol{u}), \mathcal{S}^2$ is also an underactuated balance system. We can continue to perform such a transformation. We assume that there are in total k actuated subsystems (each contains n coordinates) and (k+1)-th subsystem is fully actuated (contain last z coordinates, i.e., $m = kn + z, 0 < z < n, k, z \in \mathbb{N}$).

The S_a^i dynamics only contains the first n coordinates. S_u^i dynamics is used to obtain S^{i+1} . Hence, $S^i = \{S_a^i, S^{i+1}\}$ holds. Recursively, the S^i dynamics is written as

$$\begin{split} \mathcal{S}_{a}^{i} : D_{aa}^{(i)} q_{a}^{(i)} + D_{au}^{(i)} q_{u}^{(i)} + H_{a}^{(i)} &= B_{a}^{(i)} u, \\ \mathcal{S}_{u}^{i} &= \left\{ \mathcal{S}_{a}^{i+1}, ..., \mathcal{S}_{a}^{k}, \mathcal{S}^{k+1} \right\}, i = 0, \cdots, k \end{split}$$

where $q_u^{(i)}$ is composed by $q_a^{(i+1)}, \cdots q_a^{(k)}, q^{(k+1)}$. The original system S then is rewritten into a series of cascaded subsystems as

$$S \equiv \{S_a^0, S_a^1, S_a^2, \dots, \underbrace{S_a^k, S^{k+1}}_{S^k}\}$$

$$\underbrace{S_a^2, \dots, S_a^k, S_a^k}_{S^2}$$

$$\underbrace{S_a^2, \dots, S_a^k, S_a^k, \dots, S_a^k, S_a^k}_{S^k}$$

$$\underbrace{S_a^2, \dots, S_a^k, S_a^k, \dots, S_a^k, S_a^k, \dots, S_a^k, S_a^k, \dots, S_a^k, S_a^k, \dots, S_a^k, \dots,$$

where $\mathcal{S}_a^{k+1}=\mathcal{S}^{k+1}=\mathcal{S}_u^k.$ The original system can be viewed as $\mathcal{S}^0.$

The BEM is still used to characterize the balance target profile of each subsystem. The BEM of \mathcal{S} is obtained by using its unaccentuated subsystem. The BEM \mathcal{E}_i used as the reference trajectory of $q_a^{(i)}$ is defined

$$\mathcal{E}_{i} = \left\{ \boldsymbol{q}_{u}^{(i),e} : \boldsymbol{\Gamma}_{i} \left(\boldsymbol{q}_{a}^{(i)} ; \boldsymbol{u} \right) = \boldsymbol{0}, \dot{\boldsymbol{q}}_{a}^{(i)}, \ddot{\boldsymbol{q}}_{a}^{(i)} = \boldsymbol{0} \right\}, \quad (11)$$

where $\Gamma_i = D_{aa}^{(i)}\ddot{q}_a^{(i)} + D_{au}^{(i)}\ddot{q}_u^{(i)} + H_a^{(i)} - B_a^{(i)}u$. \mathcal{E}_i follows the BEM definition but only accounts for $q_a^{(i)}$ (i.e., n coordinates in $q_u^{(i-1)}$). While the rest of the unactuated coordinates $q_u^{(i-1)}$ is unchanged.

A. Control Design

1) Virtual Control Design: Starting from S_a^0 , we sequentially design the control input and obtain the BEM. The control input to drive $q_a^{(0)} \to q_a^{(0),d}$ is designed as

$$u_0^{\text{ext}} = \left(B_a^{(0)}\right)^{-1} \left(D_{aa}^{(0)} v_0^{\text{ext}} + D_{au}^{(0)} \ddot{q}_u^{(0)} + H_a^{(0)}\right), \quad (12)$$

where $v_0^{\text{ext}} = \ddot{q}_a^{(0),d} - a_0 e_0 - b_0 \dot{e}_0$, $e_0 = q_a^{(0)} - q_a^{(0),d}$ is the tracking error, and a_0, b_0 are control gains.

Now let's consider the general case. If the control input for \mathcal{S}^i is known, denoted as $\boldsymbol{u}_i^{\text{ext}}$, we need to design the control for \mathcal{S}^{i+1} . Within CIEC form, the immediate connection between \mathcal{S}^i and \mathcal{S}^{i+1} is the dynamics of the first n unactuated coordinates in \mathcal{S}_u^i . Therefore, we only concern the first n unactuated coordinates in $\boldsymbol{q}_u^{(i)}$ (i.e., $\boldsymbol{q}_a^{(i+1)}$).

Obtaining the BEM for $q_a^{(i+1)}$ is equivalently to inverting the \mathcal{S}_a^{i+1} dynamics under the control design $u=u_i^{\mathrm{ext}}$ and the condition $\dot{q}_a^{(i+1)}=\ddot{q}_a^{(i+1)}=0$. Precisely, we obtain BEM by solving the implicit equation $\Gamma_{i+1}=0$ and let the solution be $q_a^{(i+1),e}$. The control input is then updated to enforce $q_a^{(i+1)} \to q_a^{(i+1),e}$. We design the u_{i+1}^{ext}

$$u_{i+1}^{\text{ext}} = \left(B_a^{(i+1)}\right)^{-1} \left(D_{aa}^{(i+1)} v_{i+1}^{\text{ext}} + \bar{H}_a^{(i+1)}\right),$$
 (13)

where $ar{H}_a^{(i+1)} = D_{au}^{(i+1)} \ddot{q}_u^{(i+1)} + H_a^{(i+1)}$, $v_{i+1}^{\mathrm{ext}} = \ddot{q}_a^{(i+1),e} - a_{i+1} e_{i+1} - b_{i+1} \dot{e}_{i+1}$ is the auxiliary control and $a_{i+1}, b_{i+1} \in \mathbb{R}^{n \times n}$. The tracking error is defined as $e_{i+1} = \ddot{q}_a^{(i+1)} - \ddot{q}_a^{(i+1),e}$.

Recursively, we obtain the control design for S^{k+1} as

$$oldsymbol{u}_{k+1}^{ ext{int}} = \left(oldsymbol{B}^{(k+1)}
ight)^+ \left(oldsymbol{D}^{(k+1)} v_{k+1}^{ ext{int}} + oldsymbol{H}^{(k+1)}
ight),$$

2) Control Updating: The dynamics \mathcal{S}^k is the simplest subsystem with the property $\dim(q_a^{(k)}) \geq \dim(q_u^{(k)})$. Given the balance control u_{k+1}^{int} , incorporating the balance control of $q^{(k+1)}$ can be achieved by the EIC-based controller. Inserting u_{k+1}^{int} and v_{k+1}^{int} into \mathcal{S}^k_a dynamics leads to

$$D_{aa}^{(k)}\ddot{q}_a^{(k)} + D_{au}^{(k)}v_{k+1}^{\text{int}} + H_a^{(k)} = B_a^{(k)}u_{k+1}^{\text{int}}.$$
 (14)

Clearly, in order to achieve $q_u^{(k)}=v_{k+1}^{\mathrm{int}}$, we need to revise $q_a^{(k)}$ dynamics, which is realized by redesigning the control input

$$egin{aligned} oldsymbol{u}_k^{ ext{int}} &= \left(oldsymbol{B}_a^{(k)}
ight)^{-1} \left(oldsymbol{D}_{aa}^{(k)} oldsymbol{v}_k^{ ext{int}} + oldsymbol{D}_{au,k+1}^{(k)} oldsymbol{q}_u^{(i)} + oldsymbol{H}_a^{(k)}
ight), \ oldsymbol{v}_k^{ ext{int}} &= \left(oldsymbol{D}_{aa}^{(k)}
ight)^{-1} \left(oldsymbol{B}_a^{(k)} oldsymbol{u}_{k+1}^{ ext{int}} - oldsymbol{D}_{au,k}^{(k)} oldsymbol{v}_{k+1}^{ ext{int}} - oldsymbol{H}_a^{(k)}
ight). \end{aligned}$$

It is straightforward to verify $q_u^{(k)} = v_{k+1}^{\rm int}$ by inserting above control into (14). The control updating for $u_k^{\rm int}$ follows a similar idea in (4). Under $u_k^{\rm int}$, the balance of $q^{(k)}$ is guaranteed.

For S^i , u_i^{int} is obtained by replacing k with i. In particular, the v_i^{int} is designed to update the virtually "actuated"

coordinate $oldsymbol{q}_a^{(i+1)}$ dynamics so that it drives $oldsymbol{q}_a^{(i+1)}$ to the BEM. The control v_i^{int} is

$$\mathbf{v}_{i}^{\text{int}} = \left(\mathbf{D}_{aa}^{(i)}\right)^{-1} \left(\mathbf{B}_{a}^{(i)} \mathbf{u}_{i+1}^{\text{int}} - \mathbf{D}_{au,i+1}^{(i)} \mathbf{v}_{i+1}^{\text{int}} - \sum_{j=i+1}^{k} \mathbf{D}_{au,j+1}^{(i)} \ddot{\mathbf{q}}_{a}^{(j+1)} - \mathbf{H}_{a}^{(i)}\right)$$
(15)

for $i = 0, \dots, k$. We denote the final control as u_0^{int} . Fig. 1(b) illustrates the structure of the proposed CEIC control design. We sequentially decompose the system S^i and design control for the actuated subsystem. When updating the control input, the S^{i+1} dynamics is recognized as the internal subsystem of S^i as shown in Fig. 1(b). However, in EIC-based control, the BEM is solved at once and the updated control needs to take of all unactuated coordinates (see Fig. 1(a)). The CEIC structure takes a similar form as the backstepping control [21]. However CEIC structure is one dynamcis property of system dynamics and does not depend on the control design.

B. Stability Analysis

We show that all coordinates of \mathcal{S}^i under $oldsymbol{u}_i^{ ext{int}}$ are with active control. The convergence of the tracking error for S^i is also proved. The result in the following lemma confirms that each subsystem is under active control with the CEIC design. The proof is given in Appendix VII.

Lemma 1: Given the highly underactuated balance system S, if S can be written into the CEIC form (10), under the control input u_i^{int} , the closed-loop dynamics of \mathcal{S}^i becomes

$$\ddot{q}_a^{(j)} = v_j^{\text{int}}, \ i \leq j \leq k, \ \text{and} \ \ddot{q}^{(k+1)} = v_{k+1}^{\text{int}}.$$

$$\begin{split} \ddot{\pmb{q}}_a^{(j)} &= \pmb{v}_j^{\text{int}}, \ i \leq j \leq k, \ \text{and} \ \ \ddot{\pmb{q}}^{(k+1)} = \pmb{v}_{k+1}^{\text{int}}. \end{split}$$
 Next, we show \pmb{q} converges to $\{\mathcal{E}_i,...,\mathcal{E}_{k+1}\}$ $(\pmb{q}_a^d \ \text{is viewed}$ as \mathcal{E}_0). The control u_i^{ext} is used to obtain \mathcal{E}_{i+1} . $\Gamma_{i+1}=0$ can be explicitly written as

$$D_{au}^{(i+1)}\ddot{q}_u^{(i+1)} + H_a^{(i+1)} - B_a^{(i+1)}u_i^{\text{ext}} = 0$$
 (16)

under $x_q^{(i+1),e} = [(q_a^{(i+1)})^T \ (\ddot{q}_a^{(i+1)})^T \ (\ddot{q}_a^{(i+1)})^T]^T = [(q_a^{(i+1),e})^T \ \mathbf{0}^T \ \mathbf{0}^T]^T$. The above relationship (16) shall play a significant role in showing the convergence of $q_a^{(i)}$. The control input u_{i+1}^{int} is used to update u_i^{int} . We rewrite u_{i+1}^{int} around $x_a^{(i+1),e}$,

$$\mathbf{u}_{i+1}^{\text{int}} = \left(\mathbf{B}_{a}^{(i+1)} \right)^{-1} \left(\mathbf{D}_{au}^{(i+1)} \ddot{\mathbf{q}}_{u}^{(i+1)} + \mathbf{H}_{a}^{(i+1)} \right) \big|_{\mathbf{x}_{q}^{(i+1),e}} + o_{i}
= \left(\mathbf{B}_{a}^{(i+1)} \right)^{-1} \mathbf{B}_{a}^{(i+1)} \mathbf{u}_{i}^{\text{ext}} \big|_{\mathbf{x}_{q}^{(i+1),e}} + o_{i}
= \mathbf{u}_{i}^{\text{ext}} + o_{i},$$
(17)

where (16) is used to simplify the above equation and o_i denotes perturbations containing the higher order term and $\left(B_a^{(i+1)}\right)^{-1}D_{aa}^{(i+1)}v_{i+1}^{\operatorname{ext}}.$

To proceed, substituting (17) into $\ddot{q}_a^{(i)} = v_i^{ ext{int}}$ and using Lemma 1 yields $\ddot{q}_a^{(i)} = v_i^{\text{int}} = v_i^{\text{ext}} + O_i$, where $O_i =$ $\left(m{D}_{aa}^{(i)}
ight)^{-1}m{B}_a^{(i)}m{o}_i$. The closed-loop dynamics becomes

$$\ddot{e}_i = -a_i e_i - b_i e_i + O_i, i \le k, \tag{18a}$$

$$\ddot{e}_{k+1} = -a_{k+1}e_{k+1} - b_{k+1}e_{k+1}. \tag{18b}$$

Let $\boldsymbol{\xi} = [\boldsymbol{e}_0^T \ \dot{\boldsymbol{e}}_0^T \ \dots \ \boldsymbol{e}_{k+1}^T \ \dot{\boldsymbol{e}}_{k+1}^T]^T$ be the error vector. We rewrite the error dynamics into the following compact form

$$\mathcal{S}_e: \dot{\xi} = egin{bmatrix} 0 & I & \cdots & 0 & 0 \ -a_0 & -b_0 & \cdots & 0 & 0 \ & & \ddots & & & \ 0 & 0 & \cdots & 0 & I \ 0 & 0 & \cdots & -a_{k+1} & -b_{k+1} \end{bmatrix} oldsymbol{\xi} + egin{bmatrix} 0 \ O_0 \ dots \ 0 \ 0 \end{bmatrix} \ \hat{\Delta} egin{bmatrix} A\xi + O_{arepsilon}. \end{align}$$

We assume that the perturbation term is affine with tracking errors, that is, $\|\mathbf{O}_{\xi}\| \le c_1 \|\mathbf{\xi}\| + c_2$ for c_1 and $c_2 > 0$. If the control gains $\{a_i, b_i\}, j = i, \dots, k+1$ are properly selected such that A is Hurwitz, ξ can be shown converging to zero under perturbations. We take the Lyapunov function candidate $V = \boldsymbol{\xi}^T \boldsymbol{\xi}$ and obtain

$$\dot{V} = \boldsymbol{\xi}^{T} A \boldsymbol{\xi} + \boldsymbol{\xi}^{T} O_{\boldsymbol{\xi}} \leq \lambda_{1}(A) \|\boldsymbol{\xi}\|^{2} + \|\boldsymbol{\xi}\| (c_{1} \|\boldsymbol{\xi}\| + c_{2})$$
$$= [\lambda_{1}(A) + c_{1}] \|\boldsymbol{\xi}\|^{2} + c_{2} \|\boldsymbol{\xi}\|,$$

where $\lambda_1(A)$ denotes the greatest eigenvalue of A. If $\lambda_1(\mathbf{A}) + c_1 < 0$, the tracking error is exponentially decreasing under perturbation.

The control design is based on the CIEC form and thus the system dynamics should satisfy certain conditions. Here we summarize the conditions:

- Fully ranked matrix for each sub-order underactuated system $\operatorname{rank}(\boldsymbol{D}_{aa}^{(i)}) = \operatorname{rank}(\boldsymbol{D}_{au}^{(i)}) = \operatorname{rank}(\boldsymbol{B}_{a}^{(i)}) = n, \ i \leq k \ \text{and} \ \operatorname{rank}(\boldsymbol{D}_{aa}^{(k+1)}) = \operatorname{rank}(\boldsymbol{D}_{au}^{(k+1)}) = \operatorname{rank}(\boldsymbol{B}_{a}^{(k+1)}) = z;$
- The matrix $m{D}_{aa}^{(i+1)} m{B}_a^{(i+1)} \left(m{B}_a^{(i)}
 ight)^{-1} m{D}_{au,i+1}^{(i)}
 eq 0$ is fully ranked to guarantee that the each actuated subsystem can display the designed dynamics.

V. SIMULATION RESULTS

We present the simulation result to demonstrate and validate the proposed control design. Fig. 2 shows a tripleinverted pendulum system on a moving cart. Three joint angles and the car position are denoted as θ_i , i = 1, 2, 3, and x, respectively. With four DOFs, only the cart is actuated by external force F to follow the given reference trajectory x_d . Defining $q = [x \ \theta_1 \ \theta_2 \ \theta_3]^T$, the dynamics model is written as $D\ddot{q} + C\dot{q} + G = Bu$ [13] with u = F and

$$\boldsymbol{D} = \begin{bmatrix} M_t & -M_1 \, \mathbf{c}_1 & -M_2 \, \mathbf{c}_2 & -M_3 \, \mathbf{c}_3 \\ -M_1 \, \mathbf{c}_1 & I_1 & M_2 l_1 \, \mathbf{c}_{21} & M_3 l_1 \, \mathbf{c}_{31} \\ -M_2 \, \mathbf{c}_2 & M_2 l_1 \, \mathbf{c}_{21} & I_2 & M_3 l_2 \, \mathbf{c}_{32} \\ -M_3 \, \mathbf{c}_3 & M_3 l_1 \, \mathbf{c}_{31} & M_3 l_2 \, \mathbf{c}_{32} & I_3 \end{bmatrix},$$

$$\boldsymbol{G} = \begin{bmatrix} 0 \\ -M_1 g \, \mathbf{s}_1 \\ -M_2 g \, \mathbf{s}_2 \end{bmatrix}, \ \boldsymbol{B} = \begin{bmatrix} 1 \\ 0 \\ 0 \end{bmatrix},$$

where $s_i = \sin \theta_i$, $c_i = \cos \theta_i$, $s_{ij} = \sin(\theta_i - \theta_j)$, and $c_{ij} = \sin(\theta_i - \theta_j)$ $\cos(\theta_i - \theta_i)$. The model parameters are defined as $M_t =$ $m_c + m_1 + m_2 + m_3$, $M_1 = m_1 a_1 + (m_2 + m_3)l_1$, $M_2 =$ $m_2a_2 + m_3l_2$, $M_3 = m_3a_3$, $I_1 = J_1 + m_1a_1^2 + (m_2 + m_3)l_1^2$, $I_2 = J_2 + m_2 a_2^2 + m_3 l_2^2$, $I_3 = J_3 + m_3 a_3^2$. The length and

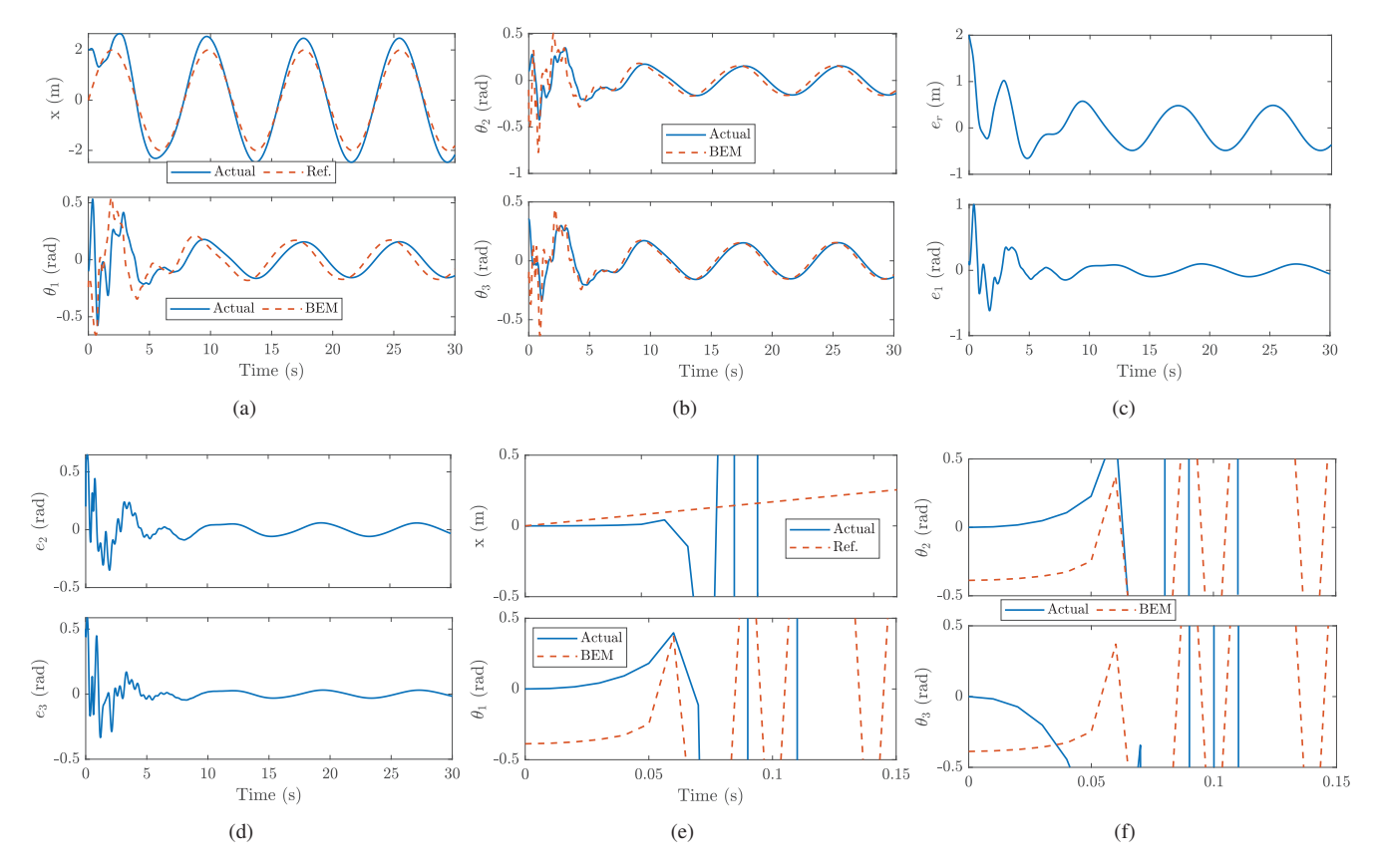


Fig. 3. Tracking control of a triple-inverted pendulum cart. (a) and (b) shows the cart position and pendulum angles under the proposed control. (c) and (d) shows the tracking errors. (e) and (f) shows the cart position and pendulum rotation angles under the EIC-based control.

distance from the joint to each link's center of mass are l_i and a_i , and the mass and the moment of inertia of each link are m_i and J_i , i=1,2,3, respectively. Variable g is the gravity constant.

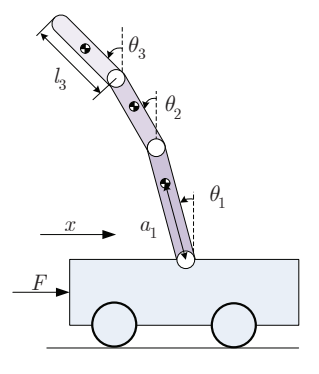


Fig. 2. Schematics of a triple-inverted pendulum on a cart. The three joints $\theta_1,\,\theta_2,\,$ and θ_3 are unactuated.

Let $q_a^{(0)} = x$, $q_a^{(1)} = \theta_1$, $q_a^{(2)} = \theta_2$, $q^{(3)} = \theta_3$, we rewrite the system dynamics into the CIEC form. For instance, \mathcal{S}_a^1 dynamics is $(J_1M_t - M_1^2\,c_1^2)\ddot{\theta}_1 + M_2(c_{21}\,l_1M_t - c_2\,c_1\,M_1)\ddot{\theta}_2 + M_3(c_{32}\,l_2M_t - c_3\,c_1\,M_1)\ddot{\theta}_3 - (M_2l_1\dot{\theta}_2^2\,s_{12} + M_3l_1\dot{\theta}_3^2\,s_{32} + M_1g\,s_1)M_t + M_1\,c_1(M_1\dot{\theta}_1^2\,s_1 + M_2\dot{\theta}_2^2\,s_2 - M_3\dot{\theta}_3^2\,s_3) = M_1\,c_1\,u$. The matrix $J_1M_t - M_1^2\,c_1^2$ and the input matrix $M_1\,c_1$ can be shown away from 0 for appropriate trajectory. The inverse of those matrixes exists. \mathcal{S}_a^2 and \mathcal{S}^3 can be obtained.

The reference trajectory of the cart is $x_d = 2\sin(0.8t)$.

TABLE I $\text{Tracking errors } (e_x=x-x_d, e_i=\theta_i-\theta_i^e, i=1,2,3) \text{ of the } \\ \text{triple-inverted pendulum}$

	$ e_x $	$ e_1 $	$ e_2 $	$ e_3 $
Absolute (m or rad)	0.31 ± 0.15	0.06 ± 0.03	0.04 ± 0.02	0.02 ± 0.01
Relative (%)	15.6 ± 7.4	35.2 ± 17.2	22.7 ± 11.1	12.4 ± 6.0

The control gains are $a_0 = 0.8, b_0 = 2.5, a_1 = 35, b_1 = 3.5, a_2 = 38, b_2 = 4.85, a_3 = 50, b_3 = 15$. The initial position of the system $q(0) = [2 - 0.1 \ 0.1 \ 0.35]^T$ is far away from the static equilibrium. Fig. 3 shows the simulation results under EIC-based control and the proposed control design. Under the CIEC-based control design, the cart follows the given reference trajectory, and all three unactuated links were kept balanced on the BEM as shown in Figs. 3(a) and 3(b). The system became unstable (see Figs. 3(e) and 3(f)) when the EIC-based control was applied, which validates the analysis in Section II. In the EIC-based control, the cart position coordinates carry the task of balancing all three links. While the CIEC-based control only assigns the task of balancing link 1 to the cart motion.

The tracking errors are shown in Figs. 3(c) and 3(d). We further summarize the steady tracking error in Table. I (mean and standard deviation). The relative error is obtained by normalizing the tracking error with the reference' (or BEM profile) amplitude. Since the system is in a cascaded form, the tracking error in the internal system would affect the

tracking performance in the external system. It is observed in Table I that $|e_1|>|e_2|>|e_3|$ in terms of the mean errors for both absolute and relative errors. The partial motion effect of $q_a^{(i)}$ serves as the control input to drive $q_a^{(i-1)}$ to its BEM. $q_a^{(2)}$ (θ_2) would not achieve the best tracking performance until the $q_a^{(3)}$ (θ_3) perfectly follows its BEM. In such a way, the task of balancing θ_3 is placed at the highest priority and all other unactuated systems are balanced one by one sequentially.

VI. CONCLUSION

This paper proposed a cascaded nonlinear control framework for highly underactuated balance robots. To achieve simultaneous trajectory tracking and balance control, the proposed framework converted a highly underactuated robot system to a series of cascaded virtually actuated subsystems. The tracking controls were sequentially designed layer-by-layer until the last subsystem. The control input was then updated from the last subsystem to the first one to incorporate the balance task. Under such a design, we showed the closed-loop system dynamics was stable. We validated the control design with numerical simulation on a triple-inverted pendulum cart system. We plan to extend such a framework with machine learning-based techniques to achieve guaranteed performance when the accurate system model is unavailable.

VII. PROOF FOR LEMMA 1

Substituting
$$u_i^{\mathrm{int}}$$
 into \mathcal{S}_a^i yields $D_{aa}^{(i)}\ddot{q}_a^{(i)}+D_{aa}^{(i)}\ddot{q}_u^{(i)}+H_a^{(i)}=B_a^{(i)}\left(B_a^{(i)}\right)^{-1}\left(D_{aa}^{(i)}v_i^{\mathrm{int}}+D_{au}^{(i)}\ddot{q}_u^{(i)}+H_a^{(i)}\right)$. After simplification, we can obtain that $\ddot{a}_a^{(i)}=v_i^{\mathrm{int}}$.

ter simplification, we can obtain that $\ddot{q}_a^{(i)} = v_i^{\text{int}}$. Next we show that \mathcal{S}_a^{i+1} under the control u_i^{int} displays the dynamics behavior $\ddot{q}_a^{(i+1)} = v_{i+1}^{\text{int}}$. Substituting u_i^{int} into \mathcal{S}_a^{i+1} yields

$$\boldsymbol{D}_{aa}^{(i+1)} \ddot{\boldsymbol{q}}_{a}^{(i+1)} + \boldsymbol{D}_{au}^{(i+1)} \ddot{\boldsymbol{q}}_{u}^{(i+1)} + \boldsymbol{H}_{a}^{(i+1)} = \boldsymbol{B}_{a}^{(i+1)} \boldsymbol{u}_{i}^{\text{int}} \quad (20)$$

The right hand side of (20) is further simplified by considering u_i^{int} as

RHS =
$$\boldsymbol{B}_{a}^{(i+1)} \left(\boldsymbol{B}_{a}^{(i)}\right)^{-1} \left(\boldsymbol{D}_{aa}^{(i)} \boldsymbol{v}_{i}^{\text{int}} + \boldsymbol{D}_{au}^{(i)} \ddot{\boldsymbol{q}}_{u}^{(i)} + \boldsymbol{H}_{a}^{(i)}\right),$$

where

$$\begin{split} \boldsymbol{B}_{a}^{(i+1)} \left(\boldsymbol{B}_{a}^{(i)}\right)^{-1} \boldsymbol{D}_{aa}^{(i)} \boldsymbol{v}_{i}^{\text{int}} \\ &= \boldsymbol{B}_{a}^{(i+1)} \boldsymbol{u}_{i+1}^{\text{int}} - \boldsymbol{B}_{a}^{(i+1)} \left(\boldsymbol{B}_{a}^{(i)}\right)^{-1} \left(\boldsymbol{D}_{au}^{(i)} \begin{bmatrix} \boldsymbol{v}_{i+1}^{\text{int}} \\ \ddot{\boldsymbol{q}}_{u}^{(i+1)} \end{bmatrix} + \boldsymbol{H}_{a}^{(i)} \right) \\ &= \boldsymbol{D}_{aa}^{(i+1)} \boldsymbol{v}_{k+1}^{\text{int}} + \boldsymbol{D}_{au}^{(i+1)} \ddot{\boldsymbol{q}}_{u}^{(i+1)} + \boldsymbol{H}_{a}^{(i+1)} \\ &- \boldsymbol{B}_{a}^{(i+1)} \left(\boldsymbol{B}_{a}^{(i)}\right)^{-1} \left(\boldsymbol{D}_{au}^{(i)} \begin{bmatrix} \boldsymbol{v}_{i+1}^{\text{int}} \\ \ddot{\boldsymbol{q}}_{u}^{(i+1)} \end{bmatrix} + \boldsymbol{H}_{a}^{(i)} \right). \end{split}$$

Thus, the right-hand side of (20) becomes

$$\begin{split} \text{RHS} = & \boldsymbol{D}_{aa}^{(i+1)} \boldsymbol{v}_{k+1}^{\text{int}} + \boldsymbol{D}_{au}^{(i+1)} \ddot{\boldsymbol{q}}_{u}^{(i+1)} + \boldsymbol{H}_{a}^{(i+1)} \\ & - \boldsymbol{B}_{a}^{(i+1)} \Big(\boldsymbol{B}_{a}^{(i)} \Big)^{-1} \boldsymbol{D}_{au}^{(i)} \begin{bmatrix} \ddot{\boldsymbol{q}}_{a}^{(i+1)} - \boldsymbol{v}_{i+1}^{\text{int}} \\ \boldsymbol{0} \end{bmatrix}. \end{split}$$

Using above equation, (20) is rewritten into

$$\left[m{D}_{aa}^{(i+1)} - m{B}_{a}^{(i+1)} \left(m{B}_{a}^{(i)}
ight)^{-1} m{D}_{au,i+1}^{(i)}
ight] \left(\ddot{m{q}}_{a}^{(i+1)} - m{v}_{i+1}^{ ext{int}}
ight) = m{0}.$$

If $D_{aa}^{(i+1)} - B_a^{(i+1)} \left(B_a^{(i)}\right)^{-1} D_{au,i+1}^{(i)}$ is fully ranked, the solution becomes $\ddot{q}_a^{(i+1)} = v_{i+1}^{\text{int}}$, which is exactly the designed control input. The proof is continued until \mathcal{S}^{k+1} . Due to the page limit, we omit the detailed derivation here.

REFERENCES

- [1] B. Karg and S. Lucia, "Efficient representation and approximation of model predictive control laws via deep learning," *IEEE Trans. Cybernetics*, vol. 50, no. 9, pp. 3866–3878, 2020.
- [2] F. Han and J. Yi, "Stable learning-based tracking control of underactuated balance robots," *IEEE Robot. Automat. Lett.*, vol. 6, no. 2, pp. 1543–1550, 2021.
- [3] E. R. Westervelt, J. W. Grizzle, and D. E. Koditschek, "Hybrid zero dynamics of planar biped walkers," *IEEE Trans. Automat. Contr.*, vol. 48, no. 1, pp. 42–56, 2003.
- [4] F. Han, X. Huang, Z. Wang, J. Yi, and T. Liu, "Autonomous bikebot control for crossing obstacles with assistive leg impulsive actuation," *IEEE/ASME Trans. Mechatronics*, vol. 27, no. 4, pp. 1882–1890, 2022.
- [5] K. Chen, Y. Zhang, J. Yi, and T. Liu, "An integrated physical-learning model of physical human-robot interactions with application to pose estimation in bikebot riding," *Int. J. Robot. Res.*, vol. 35, no. 12, pp. 1459–1476, 2016.
- [6] N. Getz, "Dynamic inversion of nonlinear maps with applications to nonlinear control and robotics," Ph.D. dissertation, Dept. Electr. Eng. and Comp. Sci., Univ. Calif., Berkeley, CA, 1995.
- [7] M. Maggiore and L. Consolini, "Virtual holonomic constraints for euler-lagrange systems," *IEEE Trans. Automat. Contr.*, vol. 58, no. 4, pp. 1001–1008, 2013.
- [8] N. Kant and R. Mukherjee, "Orbital stabilization of underactuated systems using virtual holonomic constraints and impulse controlled poincaré maps," Syst. Contr. Lett., vol. 146, 2020, article 104813.
- [9] I. Fantoni and R. Lozano and M. W. Spong, "Energy based control of pendubot," *IEEE Trans. Automat. Contr.*, vol. 45, no. 4, pp. 725–729, 2000.
- [10] K. Chen, J. Yi, and D. Song, "Gaussian-process-based control of underactuated balance robots with guaranteed performance," *IEEE Trans. Robotics*, vol. 39, no. 1, pp. 572–589, 2023.
- [11] Z. Ben Hazem, M. J. Fotuhi, and Z. Bingül, "A comparative study of the joint neuro-fuzzy friction models for a triple link rotary inverted pendulum," *IEEE Access*, vol. 8, pp. 49 066–49 078, 2020.
- [12] K. Furut, T. Ochiai, and N. Ono, "Attitude control of a triple inverted pendulum," *Int. J. Control*, vol. 39, no. 6, pp. 1351–1365, 1984.
- [13] G. A. Medrano-Cerda, "Robust stabilization of a triple inverted pendulum-cart," *Int. J. Control*, vol. 68, no. 4, pp. 849–866, 1997.
- [14] I. Crowe-Wright, "Control Theory: Double Pendulum Inverted on a Cart," Master's thesis, Dept. Mathematics and Statistics., Univ. New Mexico, Albuquerque, NM, 2018.
- [15] H. Niemann and J. Stoustrup, "Passive fault tolerant control of a double inverted pendulum — A case study," *Contr. Eng. Pract.*, vol. 13, no. 8, pp. 1047–1059, 2005.
- [16] B. Jahn, L. Watermann, and J. Reger, "On the design of stable periodic orbits of a triple pendulum on a cart with experimental validation," *Automatica*, vol. 125, 2021, article 109403.
- [17] K. Graichen, M. Treuer, and M. Zeitz, "Fast side-stepping of the triple inverted pendulum via constrained nonlinear feedforward control design," in *Proc. IEEE Conf. Decision Control*, Seville, Spain, 2005, pp. 1096–1101.
- [18] F. Han and J. Yi, "Learning-based safe motion control of vehicle ski-stunt maneuvers," in *Proc. IEEE/ASME Int. Conf. Adv. Intelli.* Mechatronics, Sapporo, Japan, 2022, pp. 724–729.
- [19] —, "On the learned balance manifold of underactuated balance robots," in *Proc. IEEE Int. Conf. Robot. Autom.*, London, UK, 2023, pp. 12254–12260.
- [20] ——, "Gaussian process-enhanced, external and internal convertible (eic) form-based control of underactuated balance robots," arXiv preprint, 2023, arXiv:2309.15784.
- [21] T. Madani and A. Benallegue, "Backstepping control for a quadrotor helicopter," in *Proc. IEEE/RSJ Int. Conf. Intell. Robot. Syst.*, 2006, pp. 3255–3260.